Approximate analytical solutions to the bidomain equations with unequal anisotropy ratios

Bradley J. Roth
Department of Physics and Astronomy, Vanderbilt University, Nashville, Tennessee 37235
(Received 11 September 1996)

The anisotropic electrical properties of cardiac tissue are described by the bidomain model. In this model, the ratio of the electrical conductivities parallel to and perpendicular to the myocardial fibers is greater in the intracellular space than in the extracellular space, resulting in a condition called unequal anisotropy ratios. No analytical solutions exist in this case. In this paper, we present approximate analytical solutions to the bidomain equations. The gist of our method is a perturbation expansion in a parameter that is defined as one minus the ratio of the anisotropy ratios in the extracellular and intracellular spaces. Three applications are considered: stimulation of the tissue by an electrode, an expanding action potential wave front, and injury currents. In the first application, the first-order perturbation term of the transmembrane potential depends on orientation by a second-order Legendre polynomial and induces adjacent regions of depolarization and hyperpolarization. In the second and third applications, the extracellular potential outside a wave front or an injured region depends on orientation by a second-order Legendre polynomial and creates regions of positive extracellular potential in the direction parallel to the fibers. [S1063-651X(97)07102-X]

PACS number(s): 87.10.+e, 87.22.Jb

I. INTRODUCTION

A better understanding of the electrical properties of cardiac tissue is essential to a better diagnosis and treatment of heart disease [1]. The *bidomain model* is a mathematical model that is often used to describe the electrical properties of cardiac tissue [2]. The bidomain equations consist of two coupled partial differential equations that govern the electrical potential in both the intracellular space (inside the cells) and the extracellular space (outside the cells). These equations are macroscopic, that is, they represent cardiac tissue as a continuum over distances on the order of 1 mm or larger. They do not account for changes of the electrical potential over microscopic distances on the order of 10 μm or less, which is the spatial scale of heart-muscle cells [3]. The intracellular and extracellular potentials should therefore be interpreted as averages over many cells, just as the macroscopic electric and magnetic fields in matter are averages over many atoms.

The bidomain equations account for anisotropy, an important characteristic of cardiac tissue. The electrical properties of cardiac tissue depend on direction because the long, thin cardiac cells tend to align themselves with their long axes parallel to each other. Moreover, the cells are coupled through intercellular channels, which tend to have greater density near the ends of the cells. Thus microscopic anatomical structure results in macroscopic anisotropy of the electrical conductivity, with this conductivity being greater along the fiber axis than perpendicular to it. Both the intracellular and extracellular spaces are anisotropic, but to different degrees [4]. In the intracellular space, the ratio of the conductivities parallel to and perpendicular to the fiber axis is about 10; in the extracellular space the ratio is about $2\frac{1}{2}$ [5]. This property of unequal anisotropy ratios leads to many surprising and important bioelectrical phenomena [6,7].

The bidomain equations do not uncouple when the tissue has unequal anisotropy ratios. Therefore, analytical solutions to the bidomain equations exist only under the artificial conditions of equal anisotropy ratios. In a preliminary report, Goel and Roth [8] proposed a perturbation method that provides approximate analytical solutions to the bidomain equations for a two-dimensional sheet of cardiac tissue with unequal anisotropy ratios. The gist of their method is a perturbation expansion in a parameter that is defined as one minus the ratio of the anisotropy ratios in the extracellular and intracellular spaces. In this paper, we extend this method and apply it to a three-dimensional volume of cardiac tissue. Then we use this technique to study three important problems in cardiac electrophysiology: stimulation by an electrode, an expanding action potential wave front, and injury currents.

II. METHODS

The intracellular potential Φ_i and the extracellular potential Φ_e are governed by the bidomain equations

$$g_{iT}\frac{\partial^2\Phi_i}{\partial x^2}+g_{iT}\frac{\partial^2\Phi_i}{\partial y^2}+g_{iL}\frac{\partial^2\Phi_i}{\partial z^2}=\beta\left[G_m(\Phi_i-\Phi_e)+C_m\frac{\partial}{\partial t}(\Phi_i-\Phi_e)\right]-I_i \quad (1)$$

and

$$g_{eT}\frac{\partial^2\Phi_e}{\partial x^2}+g_{eT}\frac{\partial^2\Phi_e}{\partial y^2}+g_{eL}\frac{\partial^2\Phi_e}{\partial z^2}=-\beta\left[G_m(\Phi_i-\Phi_e)+C_m\frac{\partial}{\partial t}(\Phi_i-\Phi_e)\right]-I_e, \quad (2)$$

where g_{iT}, g_{iL}, g_{eT}, and g_{eL} are the macroscopic electrical conductivities of the intracellular (i) and extracellular (e) spaces in the x and y directions (T, transverse) and in the z direction (L, longitudinal) (S/m). We assume that the fiber direction is uniform and that it is aligned in the z direction such that the conductivity tensors are diagonal. G_m and C_m

are the conductance and capacitance per unit area of the cell membrane (S/m^2 and F/m^2) and β is the ratio of membrane surface area to tissue volume (1/m). For the moment, we assume that G_m is a constant (passive tissue). I_i and I_e are the externally applied currents per unit volume in the intracellular and extracellular spaces (A/m^3); they represent the effect of an electrode passing current into the tissue. Equations (1) and (2) arise from the continuity of current and from Ohm's law [2,4].

In order to develop our perturbation technique, we must modify Eqs. (1) and (2). First, we replace x, y, and z with the dimensionless coordinates X, Y, and Z, where

$$X=\frac{x}{\lambda_T}, \quad Y=\frac{y}{\lambda_T}, \quad Z=\frac{z}{\lambda_L} \tag{3}$$

and the length constants in the longitudinal and transverse directions λ_L and λ_T are defined as

$$\lambda_L=\sqrt{\frac{g_{iL}g_{eL}}{(g_{iL}+g_{eL})\beta G_m}}, \quad \lambda_T=\sqrt{\frac{g_{iT}g_{eT}}{(g_{iT}+g_{eT})\beta G_m}}. \tag{4}$$

We also replace the time t by the dimensionless variable T, where

$$T=\frac{t}{\tau}, \quad \tau=\frac{C_m}{G_m}. \tag{5}$$

Next, we introduce two new variables Φ_m and Ψ to replace Φ_i and Φ_e,

$$\Phi_m=\Phi_i-\Phi_e, \quad \Psi=\Phi_i+\frac{g_{eL}}{g_{iL}}\Phi_e. \tag{6}$$

We can invert these relationships to determine Φ_i and Φ_e in terms of Φ_m and Ψ:

$$\Phi_i=\frac{g_{iL}}{g_{iL}+g_{eL}}\left(\Psi+\frac{g_{eL}}{g_{iL}}\Phi_m\right), \tag{7}$$

$$\Phi_e=\frac{g_{iL}}{g_{iL}+g_{eL}}(\Psi-\Phi_m). \tag{8}$$

The transmembrane potential Φ_m is the potential difference across the cell membrane. The transmembrane potential is important in cardiac electrophysiology because proteins embedded in a cell's membrane respond to the transmembrane potential by changing the membrane's conductance. This behavior is responsible for the nonlinear behavior of cardiac tissue, such as the propagation of action potentials. [Equations (1) and (2) contain a constant value of the membrane conductance and therefore do not include this nonlinear behavior. These equations can be generalized to model active cardiac tissue by replacing the term $G_m(\Phi_i-\Phi_e)$ with a more complicated and more realistic representation of the membrane behavior.] Ψ is an auxiliary potential with no simple physical interpretation.

Now we define two dimensionless constants α and ε,

$$\alpha=\frac{g_{iL}}{g_{eL}}, \quad \varepsilon=1-\frac{g_{eL}/g_{eT}}{g_{iL}/g_{iT}}, \tag{9}$$

and introduce the rescaled source terms

$$\gamma_i=\frac{I_i}{\beta G_m}, \quad \gamma_e=\frac{I_e}{\beta G_m}. \tag{10}$$

When the product of (g_{iT}/g_{eT}) and Eq. (2) is subtracted from Eq. (1), we obtain

$$\frac{\partial^2\Phi_m}{\partial X^2}+\frac{\partial^2\Phi_m}{\partial Y^2}+\frac{\partial^2\Phi_m}{\partial Z^2}-\Phi_m-\frac{\partial\Phi_m}{\partial T} =-\frac{\alpha\varepsilon}{1+\alpha(1-\varepsilon)}\frac{\partial^2\Psi}{\partial Z^2}+\frac{\alpha(1-\varepsilon)\gamma_e-\gamma_i}{1+\alpha(1-\varepsilon)}. \tag{11}$$

When Eq. (2) is added to Eq. (1), we obtain

$$\left(2+\alpha(1-\varepsilon)+\frac{1}{\alpha(1-\varepsilon)}\right)\left(\frac{\partial^2\Psi}{\partial X^2}+\frac{\partial^2\Psi}{\partial Y^2}\right)+\left(2+\alpha+\frac{1}{\alpha}\right)\frac{\partial^2\Psi}{\partial Z^2} =\varepsilon\left(1+\frac{1}{\alpha(1-\varepsilon)}\right)\left(\frac{\partial^2\Phi_m}{\partial X^2}+\frac{\partial^2\Phi_m}{\partial Y^2}\right)-\left(\frac{1+\alpha}{\alpha}\right)(\gamma_i+\gamma_e). \tag{12}$$

Equations (11) and (12) represent a general formulation of the bidomain equations. The introduction of the parameter ε is particularly useful. When $\varepsilon=0$, the tissue has equal anisotropy ratios. In this case, Eqs. (11) and (12) uncouple:

$$\frac{\partial^2\Phi_m}{\partial X^2}+\frac{\partial^2\Phi_m}{\partial Y^2}+\frac{\partial^2\Phi_m}{\partial Z^2}-\Phi_m-\frac{\partial\Phi_m}{\partial T}=\frac{\alpha\gamma_e-\gamma_i}{1+\alpha} \tag{13}$$

and

$$\frac{\partial^2\Psi}{\partial X^2}+\frac{\partial^2\Psi}{\partial Y^2}+\frac{\partial^2\Psi}{\partial Z^2}=-\left(\frac{1}{1+\alpha}\right)(\gamma_i+\gamma_e). \tag{14}$$

Equation (13) is the diffusion equation for Φ_m, with an additional term proportional to Φ_m that arises from the membrane conductance [in electrophysiological terms, Eq. (13) is the three-dimensional cable equation]. For steady-state situations ($\partial\Phi_m/\partial t=0$), Eq. (13) is the Helmholtz equation. Equation (14) is Poisson's equation for Ψ. Now we can see the motivation for our definition of Ψ: it leads to the complete uncoupling of the bidomain equations when $\varepsilon=0$. (Hooke *et al.* [9] discuss the relative merits of other linear combinations of Φ_i and Φ_e resulting in alternative formulations of the bidomain equations. None lead to the complete uncoupling of the bidomain equations for $\varepsilon=0$.)

The simple form of the bidomain equations for equal anisotropy ratios motivates us to perform a perturbation expansion of Φ_m and Ψ in powers of ε,

$$\Phi_m=\Phi_{m0}+\varepsilon\Phi_{m1}+\varepsilon^2\Phi_{m2}+\cdots, \tag{15}$$

$$\Psi=\Psi_0+\varepsilon\Psi_1+\varepsilon^2\Psi_2+\cdots. \tag{16}$$

When these expansions are substituted into Eqs. (11) and (12) and terms with like powers of ε are collected, we obtain

$$\nabla^2\Phi_{m0}-\Phi_{m0}-\frac{\partial\Phi_{m0}}{\partial T}=\frac{\alpha\gamma_e-\gamma_i}{1+\alpha}, \tag{17}$$

$$\nabla^2\Psi_0=-\left(\frac{1}{1+\alpha}\right)(\gamma_i+\gamma_e), \tag{18}$$

$$\nabla^2\Phi_{m1}-\Phi_{m1}-\frac{\partial\Phi_{m1}}{\partial T}=-\frac{\alpha}{1+\alpha}\frac{\partial^2\Psi_0}{\partial Z^2}-\frac{\alpha}{(1+\alpha)^2}\times(\gamma_e+\gamma_i), \tag{19}$$

$$\nabla^2\Psi_1=-\left(\frac{1-\alpha}{1+\alpha}\right)\left(\frac{\partial^2\Psi_0}{\partial X^2}+\frac{\partial^2\Psi_0}{\partial Y^2}\right)+\left(\frac{1}{1+\alpha}\right)\left(\frac{\partial^2\Phi_{m0}}{\partial X^2}+\frac{\partial^2\Phi_{m0}}{\partial Y^2}\right), \tag{20}$$

$$\nabla^2\Phi_{m2}-\Phi_{m2}-\frac{\partial\Phi_{m2}}{\partial T}=-\left(\frac{\alpha}{1+\alpha}\right)^2\frac{\partial^2\Psi_0}{\partial Z^2}-\left(\frac{\alpha}{1+\alpha}\right)\frac{\partial^2\Psi_1}{\partial Z^2}-\frac{\alpha^2}{(1+\alpha)^3}(\gamma_e+\gamma_i), \tag{21}$$

$$\nabla^2\Psi_2=-\left(\frac{1-\alpha}{1+\alpha}\right)\left(\frac{\partial^2\Psi_1}{\partial X^2}+\frac{\partial^2\Psi_1}{\partial Y^2}\right)+\left(\frac{1}{1+\alpha}\right)\left(\frac{\partial^2\Phi_{m1}}{\partial X^2}+\frac{\partial^2\Phi_{m1}}{\partial Y^2}\right)+\left(\frac{1}{1+\alpha}\right)^2\times\left(\frac{\partial^2\Phi_{m0}}{\partial X^2}+\frac{\partial^2\Phi_{m0}}{\partial Y^2}-\frac{\partial^2\Psi_0}{\partial X^2}-\frac{\partial^2\Psi_0}{\partial Y^2}\right). \tag{22}$$

Equations (17)–(22) demonstrate a way to obtain approximate analytical solutions to the bidomain equations when the solutions for equal anisotropy ratios are known. We will now use these equations to examine three important problems in cardiac electrophysiology.

III. RESULTS

A. Point source stimulation

1. Extracellular stimulation

As our first example, we will calculate the transmembrane potential distribution produced by a steady-state, extracellular point current source:

$$\gamma_i=0,\quad \gamma_e=\gamma_0\partial(X)\partial(Y)\partial(Z), \tag{23}$$

where γ_0 is the source strength and ∂ represents the Dirac delta function. This example corresponds physically to unipolar stimulation by an extracellular electrode carrying a steady current. A positive value of γ_0 corresponds to anodal stimulation and a negative value of γ_0 corresponds to cathodal stimulation. The zeroth-order solutions to the problem, Φ_{m0} and Ψ_0, correspond to equal anisotropy ratios. Φ_{m0} is the solution to the Helmholtz equation for a point source

$$\Phi_{m0}=-\gamma_0\frac{\alpha}{1+\alpha}\frac{e^{-R}}{4\pi R}, \tag{24}$$

where $R^2=X^2+Y^2+Z^2$. Ψ_0 is the solution to Poisson's equation for a point source

$$\Psi_0=\gamma_0\frac{1}{1+\alpha}\frac{1}{4\pi R}. \tag{25}$$

These solutions are equivalent to those derived previously [10,11].

Of particular interest is the first-order term of the transmembrane potential, Φ_{m1}, because this term contains the effect of unequal anisotropy ratios to lowest order. There are two source terms on the right-hand side of Eq. (19) for Φ_{m1}. One contains γ_e and gives a solution with the same spatial distribution as Φ_{m0}. The other source term is proportional to $\partial^2\Psi_0/\partial Z^2$. When expressed in spherical coordinates, the latter source term is equal to

$$-\frac{\alpha}{(1+\alpha)^2}\frac{\gamma_0}{2\pi R^3}P_2(\cos\Theta), \tag{26}$$

where $\Theta=\tan^{-1}(\sqrt{X^2+Y^2}/Z)$ and $P_2(\cos\Theta)$ is the second-order Legendre polynomial $(3\cos^2\Theta-1)/2$. The Helmholtz equation with these source terms can be solved analytically and the solution is

$$\Phi_{m1}=\frac{\alpha}{(1+\alpha)^2}\frac{\gamma_0}{6\pi}\left\{\frac{e^{-R}}{R}+\left[\frac{3}{R^3}-\frac{e^{-R}}{R}\times\left(1+\frac{3}{R}+\frac{3}{R^2}\right)\right]P_2(\cos\Theta)\right\}. \tag{27}$$

The first term amounts to a correction to the amplitude of Φ_{m0} [Fig. 1(a)]. The second term depends on Θ and gives rise to regions of both positive and negative transmembrane potential near the point source [Fig. 1(b)]. At large values of R, Φ_{m0} and the first and last terms in the expression for Φ_{m1} go to zero exponentially, so that the $1/R^3$ term in Φ_{m1} dominates. In that case, for γ_0 positive (anodal stimulation), Φ_m is positive for Θ equal to 0 or π (parallel to the fibers) and negative for Θ equal to $\pi/2$ (perpendicular to the fibers) [Fig. 1(c)]. This behavior is qualitatively similar to the result of a numerical calculation performed by Sepulveda, Roth, and Wikswo of the transmembrane potential in a two-dimensional sheet of cardiac tissue [11]. A similar transmembrane potential distribution around a unipolar stimulating electrode has been observed experimentally [12–14]. The presence of adjacent depolarized and hyperpolarized regions, implied by the $P_2(\cos\Theta)$ dependence of Φ_m, has important implications for the mechanism of stimulation [15], the shape of the virtual cathode [16], the strength-interval curve [17], and the induction of reentry and arrhythmias [18].

One advantage of an analytical solution (albeit an approximate one) over a numerical calculation is that we can easily determine how the solution depends upon the parameters of the problem. For instance, the solution for Φ_{m0} in Eq. (24) depends on α through the leading factor $\alpha/(1+\alpha)$, whereas Φ_{m1} has a leading factor of $\alpha/(1+\alpha)^2$. Because the ratio Φ_{m1}/Φ_{m0} is proportional to $1/(1+\alpha)$, we expect the effect of unequal anisotropy ratios to be greatest when α is small.

The first-order correction to Ψ is

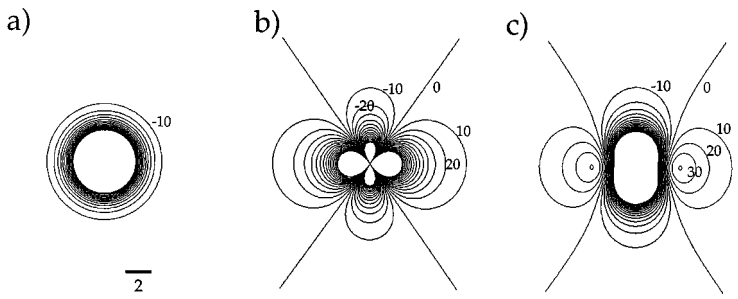

FIG. 1. Transmembrane potential induced by a point extracellular current source. The electrode is at the center of the plot. The fiber direction and Z axis are horizontal. The bar denotes two space units and contours are drawn every 10 mV. $\varepsilon=\frac{3}{4}$, $\alpha=1$, and $\gamma_0=156$ V (corresponding to 1-mA stimulation). Contours for very large potentials near the electrode are not drawn. (a) Φ_{m0} [Eq. (24)] plus the part of Φ_{m1} that is independent of Θ [Eq. (27)], (b) the part of Φ_{m1} that is proportional to $P_2(\cos\Theta)$ [Eq. (27)], and (c) $\Phi_{m0}+\Phi_{m1}$.

$$\Psi_1=-\frac{\gamma_0}{6\pi}\frac{1-\alpha}{(1+\alpha)^2}\left[\frac{1}{R}+\frac{1}{2R}P_2(\cos\Theta)\right]+\frac{\gamma_0}{6\pi}\frac{\alpha}{(1+\alpha)^2}\times\left\{-\frac{e^{-R}}{R}+\left[-\frac{3}{R^3}+\frac{e^{-R}}{R}\left(1+\frac{3}{R}+\frac{3}{R^2}\right)\right]\times P_2(\cos\Theta)\right\}. \tag{28}$$

The first term in this equation has the same spatial distribution as Ψ_0 and it therefore provides a first-order correction to the amplitude. The second term is more interesting because of the Θ dependence. At large values of R, this term contributes significantly to Ψ_1, but because Ψ_0 does not vanish, the term supplies only a first-order correction to the behavior of Ψ. For large values of R and through first order, Φ_m falls off as $1/R^3$, whereas Ψ falls off as $1/R$. Therefore, $\Psi\gg\Phi_m$ at large values of R, and Φ_i and Φ_e are nearly proportional to Ψ. For equal anisotropy ratios, Φ_i and Φ_e would have spherical isocontours at large values of R (they would be elliptical if plotted as functions of x, y, and z). Ψ_1 causes the contours to deviate from this spherical shape, but this is a first-order deviation and it is therefore small.

2. Intracellular stimulation

Intracellular stimulation, which is possible by means of microelectrodes, corresponds to

$$\gamma_i=-\gamma_0\partial(X)\partial(Y)\partial(Z),\quad \gamma_e=0. \tag{29}$$

The minus sign in this expression ensures that a positive value of γ_0 will correspond to hyperpolarization of the tissue (negative Φ_m) under the electrode. The solution for Φ_m and Ψ is analogous to our previous result:

$$\Phi_{m0}=-\gamma_0\frac{1}{1+\alpha}\frac{e^{-R}}{4\pi R}, \tag{30}$$

$$\Psi_0=-\gamma_0\frac{1}{1+\alpha}\frac{1}{4\pi R}, \tag{31}$$

$$\Phi_{m1}=-\frac{\alpha}{(1+\alpha)^2}\frac{\gamma_0}{6\pi}\left\{\frac{e^{-R}}{R}+\left[\frac{3}{R^3}-\frac{e^{-R}}{R}\times\left(1+\frac{3}{R}+\frac{3}{R^2}\right)\right]P_2(\cos\Theta)\right\}, \tag{32}$$

and

$$\Psi_1=\frac{\gamma_0}{6\pi}\frac{1-\alpha}{(1+\alpha)^2}\left[\frac{1}{R}+\frac{1}{2R}P_2(\cos\Theta)\right]+\frac{\gamma_0}{6\pi}\frac{1}{(1+\alpha)^2}\times\left\{-\frac{e^{-R}}{R}+\left[-\frac{3}{R^3}+\frac{e^{-R}}{R}\left(1+\frac{3}{R}+\frac{3}{R^2}\right)\right]\times P_2(\cos\Theta)\right\}. \tag{33}$$

Note that Φ_{m0} does not change signs when going from extracellular to intracellular stimulation, but Φ_{m1} does. For intracellular stimulation that hyperpolarizes the tissue near the electrode, there are regions of depolarization in the direction perpendicular to the fiber axis (as opposed to regions of depolarization parallel to the fiber axis caused by extracellular stimulation).

Sepulveda, Roth, and Wikswo [11] considered the case in which intracellular and extracellular stimulation were both applied at the same position with equal and opposite strength:

$$\gamma_i=-\gamma_0\partial(X)\partial(Y)\partial(Z),\quad \gamma_e=\gamma_0\partial(X)\partial(Y)\partial(Z). \tag{34}$$

The solution follows from superposition of our two previous results:

$$\Phi_{m0}=-\gamma_0\frac{e^{-R}}{4\pi R}, \tag{35}$$

$$\Psi_0=0, \tag{36}$$

$$\Phi_{m1}=0, \tag{37}$$

$$\Psi_1=\frac{\gamma_0}{6\pi}\frac{1}{(1+\alpha)^2}\left\{-\frac{e^{-R}}{R}+\left[-\frac{3}{R^3}+\frac{e^{-R}}{R}\times\left(1+\frac{3}{R}+\frac{3}{R^2}\right)\right]P_2(\cos\Theta)\right\}. \tag{38}$$

Ψ_1 has no $1/R$ term and has a spatial distribution similar to that of Φ_m for intracellular stimulation.

To first order, Φ_m is spherically symmetric. An angular dependence is present in the second-order term for the transmembrane potential. The full solution for Φ_{m2} is rather complicated, but one term dominates at $R\gg1$:

$$\Phi_{m2} = -\gamma_0 \frac{6}{\pi} \frac{\alpha^2}{(1+\alpha)^3} \frac{1}{R^5} P_4(\cos\Theta), \tag{39}$$

where $P_4(\cos\Theta)$ is the fourth-order Legendre polynomial $(35\cos^4\Theta - 30\cos^2\Theta + 3)/8$. During cathodal stimulation ($\gamma_0 < 0$), Φ_{m2} causes hyperpolarized regions in the directions that are approximately 45° from the fiber axis and depolarized regions in the directions parallel to and perpendicular to the fiber axis. These conclusions are consistent with the numerical calculations of Sepulveda, Roth, and Wikswo [11] (see their Fig. 8).

B. Expanding wave front

Another important problem in cardiac electrophysiology is the calculation of the extracellular potential that is produced by an expanding action-potential wave front. Many cardiac arrhythmias are caused by abnormal propagation of wave fronts through the heart and often the clinician needs to determine the path of propagation before deciding on the appropriate therapy. Although the transmembrane potential contains the most useful information about wave-front propagation, the extracellular potential is much easier to measure. Often the clinician desires to learn about Φ_m from measurements of Φ_e.

We will now consider a spherical wave front (ellipsoidal in x, y, and z coordinates) that is propagating outward. In this example, there are no applied sources; therefore, γ_i and γ_e are equal to zero. (We will not concern ourselves with how this wave front originated; we will assume that the sources that initiated it are no longer active). The membrane is not passive and the active ion channels in the membrane provide the source of the extracellular potential. We cannot solve this problem completely with the passive theory developed above. However, we can make some progress by realizing that the leading edge of a cardiac wave front (the ''depolarization'' front) is very thin and the tissue is nearly passive both in front of it and behind it. (The cardiac action potential has a rise time of about 1 ms, followed by a plateau lasting over 100 ms.)

We will assume that the wave front can be treated as a step function; therefore, the transmembrane potential is zero ahead of the wave front and V_0 behind it. Consequently, we take the zeroth-order expansion of the transmembrane potential to be

$$\Phi_{m0} = \begin{cases} V_0, & R < R_0 \\ 0, & R > R_0 . \end{cases} \tag{40}$$

Because there are no applied sources, $\Psi_0 = 0$ everywhere. We see from Eq. (19) that both source terms for Φ_{m1} are equal to zero. Thus unequal anisotropy ratios does not lead to a first-order correction to our assumed wave front ($\Phi_{m1} = 0$). The second source term in Eq. (20) for Ψ_1 is not equal to zero, however. In this case, Eq. (20) can be solved analytically, yielding

$$\Psi_1 = \frac{1}{1+\alpha} \frac{2}{3} V_0 \times \begin{cases} 1, & R < R_0 \\ \left(\frac{R_0}{R}\right)^3 P_2(\cos\Theta), & R > R_0 . \end{cases} \tag{41}$$

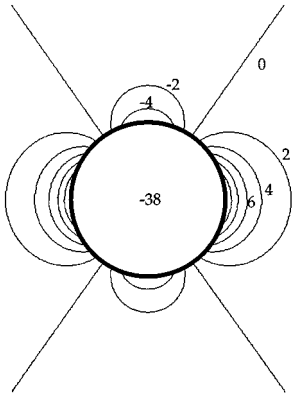

FIG. 2. Extracellular potential (accurate to first order) induced by an expanding action potential wave front [Eq. (42)]. The position of the wave front corresponds to the bold circle. The fiber direction and the Z axis are horizontal. Contours are drawn every 2 mV. $\varepsilon = \frac{3}{4}$, $\alpha = 1$, $V_0 = 100$ mV, and $R_0 = 4$.

The extracellular potential is given in terms of Φ_m and Ψ in Eq. (8). We can write the extracellular potential, to first order in ε, as (see Fig. 2)

$$\Phi_e = \frac{\alpha}{1+\alpha} V_0 \times \begin{cases} -1 + \varepsilon \frac{2}{3} \frac{1}{1+\alpha}, & R < R_0 \\ \varepsilon \frac{1}{1+\alpha} \frac{2}{3} \left(\frac{R_0}{R}\right)^3 P_2(\cos\Theta), & R > R_0 . \end{cases} \tag{42}$$

If the tissue had equal anisotropy ratios ($\varepsilon = 0$), the extracellular potential outside a closed, expanding wave front would vanish. (This phenomenon corresponds to the ''uniform double layer'' model often referred to in the electrocardiology literature [19].) But unequal anisotropy ratios induce a part of the extracellular potential that has the spatial distribution of a second-order Legendre polynomial. In the directions parallel to the fibers ($\Theta = 0°, 180°$), the extracellular potential outside the wave front is positive; in the directions perpendicular to the fibers ($\Theta = 90°, 270°$), the extracellular potential is negative. This distribution of extracellular potential has been computed numerically [20] and observed experimentally [21,22].

The second-order correction term to the transmembrane potential Φ_{m2} does not vanish [Eq. (21)]. The entire solution to the Φ_{m2} problem is rather difficult, but a particular solution Φ^*_{m2} can be readily calculated

$$\Phi^*_{m2} = \frac{\alpha}{(1+\alpha)^2} \frac{8V_0}{R_0^2} \times \begin{cases} 0, & R < R_0 \\ \left(\frac{R_0}{R}\right)^5 P_4(\cos\Theta), & R > R_0 . \end{cases} \tag{43}$$

Because the homogeneous solution to Eq. (21) rapidly falls off in space, the particular solution should make the dominant contribution to Φ_{m2} at more than a few length constants from the wave front ($|R - R_0| \gg 1$). The angular dependence

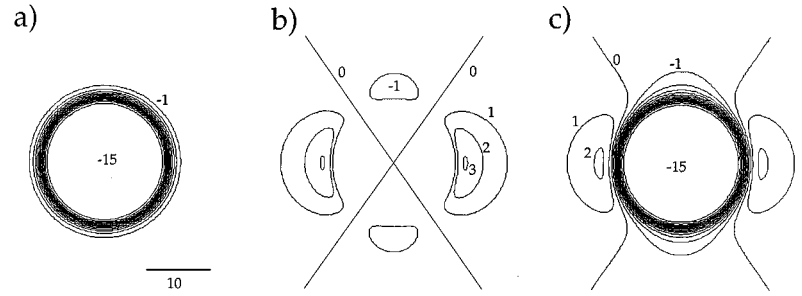

FIG. 3. Extracellular potential induced by an injured region [Eqs. (52) and (55)]. The fiber direction and the Z axis are horizontal. Contours are drawn every millivolt. $\varepsilon=\frac{3}{4}$, $\alpha=1$, $E=50$ mV, $G=4$, and $R_0=10$. (a) Φ_{e0} plus the part of Φ_{e1} that is independent of Θ, (b) the part of Φ_{e1} that is proportional to $P_2(\cos\Theta)$, and (c) $\Phi_{e0}+\Phi_{e1}$.

of $P_4(\cos\Theta)$ implies that Φ_{m2} is positive at $\Theta=0°$, 90°, 180°, and 270°. It is negative along the diagonal directions (at $\Theta=45°$, 135°, 225°, and 315°). Because the effect is second order in ε, the magnitude of Φ_{m2} is small. In addition, the magnitude of Φ_{m2} falls off as $1/R_0^2$, making this effect larger for highly curved wave fronts and smaller for nearly flat wave fronts ($R_0 \gg 1$). Using a numerical calculation, Pollard, Hooke, and Henriquez [23] predicted regions of hyperpolarization leading an outwardly propagating wave front in the directions 45° from the fiber axis. Our results are in qualitative agreement with their prediction.

C. Injury currents

A third significant problem in cardiac electrophysiology is the response of the heart to a localized region of tissue with abnormal electrical properties (i.e., ''injured'' tissue). If the injured region remains coupled to the surrounding tissue, steady-state currents (''injury currents'') can arise between the injured and the normal tissue. The same idea applies to healthy tissue that has a local modification of the cell membrane's electrical properties (e.g., response to local application of a neurotransmitter). This problem is also important when we consider the response of smooth muscle to transmitter secretion. Poznanski [24] has studied this problem using the bidomain model, but only for the case of equal anisotropy ratios. We can use our perturbation technique to generalize his result to unequal anisotropy ratios.

We start with the bidomain equations [Eqs. (1) and (2)] but we add an additional term to represent a region of leaky membrane. We assume that the tissue is in steady state, no applied currents exist ($\gamma_i=\gamma_e=0$), the leaky region lies within a sphere of radius R_0 centered at the origin (within an ellipsoid in x, y, and z coordinates), the leaky membrane has a conductance per unit area of G_m^* in parallel with the normal membrane conductance G_m, and the leaky membrane conductance G_m^* has a reversal potential of E. (In our previous calculations, we neglected the resting potential, which is the steady-state potential difference of about -80 mV that exists between the intracellular and extracellular space in normal, resting cardiac tissue. If we had included the resting potential, then E would represent the difference between the resting potential within the cell and the ground outside the cell. In other words, the leaky membrane represents the effect of non-selective pores in the membrane that tend to reduce the resting potential toward zero.)

With these assumptions, we can write the bidomain equations as

$$\frac{\partial^2\Phi_m}{\partial X^2}+\frac{\partial^2\Phi_m}{\partial Y^2}+\frac{\partial^2\Phi_m}{\partial Z^2}-\Phi_m = -\frac{\alpha\varepsilon}{1+\alpha(1-\varepsilon)}\frac{\partial^2\Psi}{\partial X^2}+H(R,R_0)\frac{G_m^*}{G_m}(\Phi_m-E) \tag{44}$$

and

$$\left(2+\alpha(1-\varepsilon)+\frac{1}{\alpha(1-\varepsilon)}\right)\left(\frac{\partial^2\Psi}{\partial X^2}+\frac{\partial^2\Psi}{\partial Y^2}\right)+\left(2+\alpha+\frac{1}{\alpha}\right)\frac{\partial^2\Psi}{\partial Z^2} =\varepsilon\left(1+\frac{1}{\alpha(1-\varepsilon)}\right)\left(\frac{\partial^2\Phi_m}{\partial X^2}+\frac{\partial^2\Phi_m}{\partial Y^2}\right), \tag{45}$$

where

$$H(R,R_0)=\begin{cases}1, & R<R_0\\ 0, & R>R_0.\end{cases} \tag{46}$$

Using $G=G_m^*/G_m$ and performing our perturbation expansion, we get

$$\nabla^2\Phi_{m0}-(1+GH)\Phi_{m0}=-GHE, \tag{47}$$

$$\nabla^2\Psi_0=0, \tag{48}$$

$$\nabla^2\Phi_{m1}-(1+GH)\Phi_{m1}=-\frac{\alpha}{1+\alpha}\frac{\partial^2\Psi_0}{\partial Z^2}, \tag{49}$$

$$\nabla^2\Psi_1=\left(\frac{1}{1+\alpha}\right)\left(\frac{\partial^2\Phi_{m0}}{\partial X^2}+\frac{\partial^2\Phi_{m0}}{\partial Y^2}\right), \tag{50}$$

$$\nabla^2\Phi_{m2}-(1+GH)\Phi_{m2}=-\left(\frac{\alpha}{1+\alpha}\right)\frac{\partial^2\Psi_1}{\partial Z^2}. \tag{51}$$

The solution to Eq. (47) for Φ_{m0} is [see Fig. 3(a)]

$$\Phi_{m0}=\frac{G}{1+G}E\times\begin{cases}1+A\dfrac{\sinh(R\sqrt{1+G})}{R}, & R<R_0\\ B\dfrac{e^{-R}}{R}, & R>R_0.\end{cases} \tag{52}$$

The constants A and B can be determined from the continuity of Φ_{m0} and its radial derivative at $R=R_0$,

$$A=-\frac{R_0}{\sinh(R_0\sqrt{1+G})}\left[\frac{1}{1-[1-\sqrt{1+G}R_0\coth(R_0\sqrt{1+G})]/(1+R_0)}\right], \tag{53}$$

$$B=\frac{R_0}{e^{-R_0}}\left[\frac{1}{1-(1+R_0)/[1-\sqrt{1+G}R_0\coth(R_0\sqrt{1+G})]}\right]. \tag{54}$$

The solutions to Eq. (48) for Ψ_0 and Eq. (49) for Φ_{m1} vanish (there is no first-order correction term to the transmembrane potential). The solution to Eq. (50) for Ψ_1 is [see Fig. 3(b)]

$$\Psi_1=\frac{2}{3}\frac{1}{1+\alpha}\frac{G}{1+G}E \times\begin{cases} A\dfrac{\sinh(R\sqrt{1+G})}{R}+1-\dfrac{A}{1+G}\left[\left(\dfrac{1+G}{R}+\dfrac{3}{R^3}\right)\sinh(R\sqrt{1+G})-\dfrac{3\sqrt{1+G}}{R^2}\cosh(R\sqrt{1+G})\right]P_2(\cos\Theta) \\ B\dfrac{e^{-R}}{R}-B\dfrac{e^{-R}}{R}\left(1+\dfrac{3}{R}+\dfrac{3}{R^2}\right)P_2(\cos\Theta)+C\left(\dfrac{R_0}{R}\right)^3P_2(\cos\Theta), \end{cases} \tag{55}$$

where C is given by

$$C=1+\frac{3}{R_0^2}\frac{G}{1+G} \times\frac{1}{1/(1+R_0)-1/[\sqrt{1+G}R_0\coth(R_0\sqrt{1+G})]}. \tag{56}$$

At large values of R ($R-R_0\gg1$), the only term that contributes significantly to Ψ_1 is the last term, which has a $P_2(\cos\Theta)$ angular dependence [Fig. 3(c)]. Thus extracellular potentials measured outside the injured tissue will have a distinctive directional dependence, similar to that observed outside an expanding wave front. This directional dependence needs to be taken into account when extracellular potential measurements are used to deduce the transmembrane potential distribution [25].

By analogy with the expanding wave-front problem, there will be a nonzero Φ_{m2} that has a $P_4(\cos\Theta)$ angular dependence. Because the Φ_{m2} contribution is second order, it will be small in relation to Φ_{m0}, except at $R\gg R_0$.

IV. DISCUSSION

In this paper, we developed a perturbation technique for studying the electrical properties of cardiac tissue, with an emphasis on the tissue anisotropy. Perturbation methods and similar multiscale techniques are not new to theoretical cardiac electrophysiology. Neu and Krassowska [3] used a multiscale method to derive the bidomain equations from a microscopic model of the tissue's cellular structure. Keener [26] and Colli-Franzone, Guerri, and Rovida [27] used multiscale techniques to derive eikonal equations that govern the speed of propagation of action potential wave fronts. These previous studies differ from ours in a fundamental way. The difference can best be appreciated by examining the ''small parameter'' used in the perturbation theory. Neu and Krassowska used a small parameter equal to the ratio of the cell diameter to the tissue length constant and examined effects arising from the discrete cellular nature of the tissue. Keener's and Colli-Franzone, Guerri, and Rovida's small parameter arose from assuming that the conductivity of cardiac tissue changed slowly over distances on the order of the depolarization wave-front thickness. They also examined changes in propagation velocity with fiber curvature and rotation. All three of these methods examine changes in tissue properties in space (inhomogeneities), on either a large or a small spatial scale. Our perturbation method, on the other hand, examines the electrical behavior of a continuous, homogeneous tissue. Our small parameter ε arises from the inherent nature of the tissue anisotropy, not from any inhomogeneity. It gives rise to effects that are completely different from those found during previous studies of cardiac tissue using perturbation methods.

One virtue of our perturbation method is that it elucidates which properties of cardiac tissue arise from unequal anisotropy ratios and which do not. First-order effects include adjacent regions of depolarization and hyperpolarization near a stimulating electrode and directional dependence of the extracellular potential outside an expanding action potential wave front or a region of injury. The first two of these effects have been observed experimentally.

The key parameter in our analysis is ε, which is equal to one minus the ratio of the anisotropy ratios in the extracellular and intracellular space. For our perturbation analysis to be most useful, ε should be small. Experiments indicate, however, that ε has a value of about 0.75, which is not exceptionally small [5]. Thus, while first-order terms in our perturbation expansion provide great insight into the qualitative electrical behavior of cardiac tissue, a quantitative analysis may require the inclusion of higher-order terms in the expansion.

ACKNOWLEDGMENTS

We thank Barry Bowman for a critical reading of the manuscript and Vivek Goel for his assistance in developing a preliminary version of this work. This research was supported by the Whitaker Foundation; the American Heart Association–Tennessee Affiliate; and the College of Arts & Science, Vanderbilt University.

[1] D. P. Zipes and J. Jalife, *Cardiac Electrophysiology, From Cell to Bedside*, 2nd ed., edited by D. P. Zipes and J. Jalife (Saunders, Philadelphia, 1995).
[2] C. S. Henriquez, Crit. Rev. Biomed. Eng. **21**, 1 (1993).
[3] J. C. Neu and W. Krassowska, Crit. Rev. Biomed. Eng. **21**, 137 (1993).
[4] B. J. Roth, J. Math. Biol. **30**, 633 (1992).
[5] B. J. Roth, IEEE Trans. Biomed. Eng. (to be published).
[6] J. P. Wikswo, Jr., in *Cardiac Electrophysiology, From Cell to Bedside* (Ref. [1]), p. 348.
[7] B. J. Roth and J. P. Wikswo, Jr., Proc. IEEE **84**, 379 (1996).
[8] V. Goel and B. J. Roth, in *Proceedings of the 13th Southern Biomedical Engineering Conference*, edited by J. Vossoughi (Engineering Research Center, Washington, D.C., 1994), p. 967.
[9] N. Hooke *et al.*, Math. Biosci. **120**, 127 (1994).
[10] R. Plonsey and R. Barr, IEEE Trans. Biomed. Eng. **29**, 541 (1982).
[11] N. G. Sepulveda, B. J. Roth, and J. P. Wikswo, Jr., Biophys. J. **55**, 987 (1989).
[12] M. Neunlist and L. Tung, Biophys. J. **68**, 2310 (1995).
[13] S. B. Knisley, Circ. Res. **77**, 1229 (1995).
[14] J. P. Wikswo, Jr., S.-F. Lin, and R. A. Abbas, Biophys. J. **69**, 2195 (1995).
[15] B. J. Roth, IEEE Trans. Biomed. Eng. **42**, 1174 (1995).
[16] B. J. Roth and J. P. Wikswo, Jr., IEEE Trans. Biomed. Eng. **41**, 232 (1994).
[17] B. J. Roth, J. Cardiovasc. Electrophysiol. **7**, 722 (1996).
[18] J. M. Saypol and B. J. Roth, J. Cardiovasc. Electrophysiol. **3**, 558 (1992).
[19] E. Frank, Am. Heart J. **46**, 364 (1953).
[20] N. G. Sepulveda and J. P. Wikswo, Jr., Biophys. J. **51**, 557 (1987).
[21] L. V. Corbin and A. M. Scher, Circ. Res. **41**, 58 (1977).
[22] P. Colli-Franzone *et al.*, Circ. Res. **51**, 330 (1982).
[23] A. E. Pollard, N. Hooke, and C. S. Henriquez, in *High Performance Computing in Biomedical Research*, edited by T. Pilkington *et al.* (CRC, Boca Raton, FL, 1993), p. 319.
[24] R. R. Poznanski, Ann. Biomed. Eng. **21**, 401 (1993).
[25] M. R. Bennett, W. G. Gibson, and R. R. Poznanski, Philos. Trans. R. Soc. London Ser. B **342**, 89 (1993).
[26] J. P. Keener, J. Math. Biol. **29**, 629 (1991).
[27] P. Colli-Franzone, L. Guerri, and S. Rovida, J. Math. Biol. **28**, 121 (1990).